



April/May 2013 • Volume 5 • Issue 2 (Published since 2009)

Special Issue

Reliability of Multilayer Ceramic Capacitors with Base-Metal Electrodes

Base-metal electrode (BME) multilayer ceramic capacitors have drawn much recent attention. This special issue of the *EEE Parts Bulletin* was written by David (Donhang) Liu, a capacitor specialist at NASA Goddard Space Flight Center.

1. Capacitor Reliability and System Reliability

Multilayer ceramic capacitors (MLCCs) are key building blocks in modern electronics. MLCCs comprise ~30% of the total components in a typical hybrid circuit module such as a DC-DC converter. The numbers of ceramic capacitors used in integrated circuit (IC) power supply decoupling applications are even greater. Figure 1 shows an example of today's large-scale IC chip package with many decoupling BME MLCCs around it. Due to the demand for increasing numbers of decoupling capacitors and the limited space available, the use of BME capacitors with higher capacitance and a smaller chip size is more attractive for current large-scale IC chip packages.

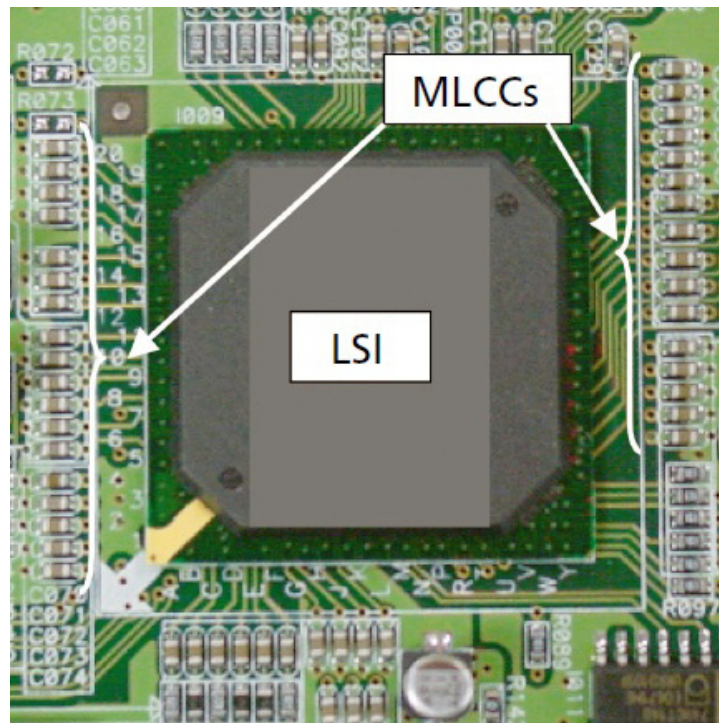


Figure 1. MLCC application in a large-scale integrated circuit showing MLCCs around the periphery of a large-scale integration (LSI) package.

Indeed, a typical Intel central processing unit (CPU) package today requires more than 100 ceramic capacitors performing a variety of functions related to power delivery and signal integrity. These capacitors all need to work reliably for the CPU to function. Due to cost pressures, the degree of redundancy in CPU systems has been reduced, and so the failure of even one capacitor can cause the whole system to fail.

Capacitor reliability is vital for all electronic systems, which may help to explain why the NASA Electronic Parts and Packaging (NEPP) program has continuously funded studies on the reliability issues of various capacitor technologies.

In its simplest form, the capacitor system reliability can be expressed as:

$$\text{Capacitor system reliability} = \text{component reliability}^{\text{Number of capacitors}}$$

If a CPU system with 100 capacitors needs to maintain a system reliability of 99.9%, each capacitor must have an individual component reliability of 99.999%.

2. Characteristics of Multilayer Ceramic Capacitors

An MLCC is a high-temperature (1350°C typical) co-fired ceramic monolithic that is composed of many layers of alternately stacked oxide-based dielectrics and internal metal electrodes. The internal electrodes are connected in parallel to form end terminations for the electrical contacts (Figure 2).

The capacitance C_t of an MLCC can be represented by:

$$C = \epsilon_r \cdot \epsilon_0 \cdot N \cdot \frac{S}{d}, \quad (1)$$

where S is the overlap area of internal electrodes, N is the number of individual dielectric layers, ϵ_r is the relative dielectric constant of the ceramic dielectric, d is the thickness of the dielectric layer, and ϵ_0 is the dielectric constant of free space.

Another important parameter for measuring the degree of miniaturization of a capacitor is *volumetric efficiency*, which is the capacitance per volume and which can be expressed as:

$$\frac{C_t}{V} \approx \epsilon_0 \frac{\epsilon_r}{d^2} \approx 8.854 \times 10^{-8} \frac{\epsilon_r}{d^2} \left(\frac{\mu F}{cm^3} \right), \quad (2)$$

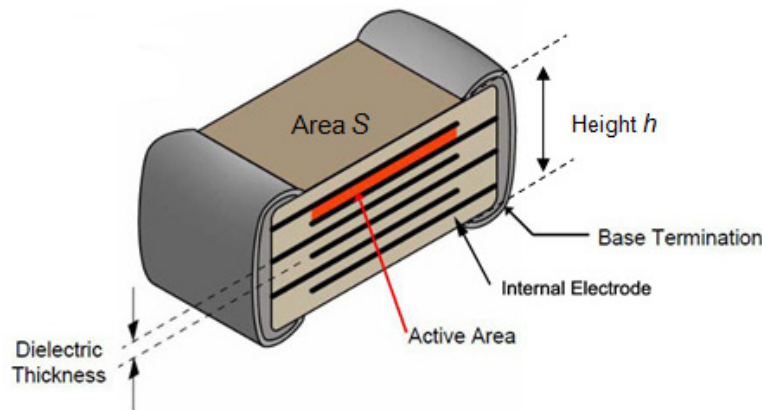


Figure 2. Typical structure of an MLCC device.

where ϵ_r is the dielectric constant and d is the dielectric thickness. MLCCs with high volumetric efficiency can be achieved by increasing the dielectric constant and reducing the dielectric thickness.

3. Precious-Metal Electrodes vs. Base-Metal Electrodes

During the manufacturing of MLCC products, in order to make the dielectric layers insulating and the metal electrode layers conducting, only highly oxidation-resistant precious metals such as platinum, palladium, and silver can be used for the co-firing in a regular air atmosphere. MLCCs made with precious metals as internal electrodes and terminations are called precious-metal electrode (PME) capacitors. To date, MIL-PRF-123 requires all MLCCs for high-reliability and space projects to be PME capacitors.

In the early 1990s, the high cost of precious metal materials, coupled with uncertainty about their continued availability, forced an industry shift from PME to BME (Ni, Cu) technology for most commercial MLCCs. The switch from PMEs to BMEs required a change in the manner in which the ceramic is fired from a regular-air atmosphere to a reducing atmosphere (low oxygen) to prevent the oxidation of internal nickel electrodes. This creates a significant amount of oxygen vacancies in the dielectric that will migrate under DC bias and degrade the dielectric's insulating resistance. After more than two decades of development, the insulating resistance degradation in BME MLCCs has been significantly reduced by two primary approaches: (1) a subsequent low-temperature firing in an oxygen-rich environment to re-oxidize the dielectric by occupying the oxygen vacancies, and (2) rare-earth element doping to pin or slow down the migration of still-existing oxygen vacancies.

Although issues and concerns remain with respect to the lifetime reliability of MLCCs manufactured using BME technology, substantial progress has been made. Due to its improved voltage robustness and its capability for making more layers of internal electrodes, some BME capacitors can achieve lifetime reliability equal to or better than that of space-level PME capacitors, with higher capacitance per volume (*volumetric efficiency*) and much lower cost. This is another advantage to using BME capacitors for high-reliability, space-level applications.

An investigation into the possible use of BME capacitors for high-reliability NASA space-level applications has become urgent and inevitable.

4. Reliability of BME Capacitors

The evaluation of BME capacitors for potential NASA space project applications requires an in-depth understanding of the reliability of BME capacitors. BME capacitors cannot be qualified for high reliability; they must be made for it.

4.1 Reliability of MLCCs

The reliability of an MLCC is the ability of the dielectric material to retain its insulating properties under stated environmental and operational conditions for a specified period of time t . A general expression of reliability consists of three parts and can be expressed as:

$$R(t) = \varphi(N, d, \bar{r}, S) \times AF(V, T) \times \gamma(t), \quad (3)$$

where $\gamma(t)$ is a statistical distribution that describes the individual variation of properties in a testing group of samples (Weibull, log normal, normal, etc.).

$AF(V, T)$ is an acceleration function that describes how a capacitor's reliability responds to external stresses such as applied voltage V and temperature T . All units in the testing group should follow the same acceleration function if they share the same failure mode (independent of individual units).

$\varphi(N, d, \bar{r}, S)$ describes the effect on reliability of the structural and constructional characteristics of a capacitor device, such as the number of dielectric layers N , the dielectric thickness d , average grain size \bar{r} , and capacitor chip size S .

In general, a two-parameter Weibull statistical distribution model is often used in the description of a BME capacitor's reliability as a function of time:

$$\gamma(t) = e^{-\left(\frac{t}{\eta}\right)^\beta}, \quad (4)$$

where e is the base for natural logarithms, β is the dimensionless *slope* parameter whose value is often characteristic of the particular failure mode under study, and η is the *scale* parameter that represents a characteristic time at which 63.2% of the population has failed and that is related to all other characteristic times, such as mean time to failure (MTTF):

$$MTTF = \eta \Gamma(1 + 1/\beta), \quad (5)$$

where $\Gamma(x)$ is the gamma function of x (Note: $\Gamma(1+1/\beta) \approx 0.9$ when $\beta > 3.0$).

Equation (4) provides a simple and clear understanding of the meaning of reliability:

Reliability is a monotonic function of time and always decreases with time, which indicates that the loss of reliability is a common behavior for all devices.

Since η and β always exceed zero, the value of $R(t)$ is always between 0 and 1, indicating that reliability can also be viewed as the probability of a failure to occur.

Reliability typically defines the durability of a system that can function normally. When $\beta > 3$ and $t < \eta$, $R(t) \sim 1$, suggesting a reliable life span before η . When $t > \eta$, $R(t)$ decreases rapidly to 0. The lifetime of a device to sustain its function can be characterized by η , as shown in Eq. (5).

4.2 Acceleration Functions of BME Capacitors

$AF(V, T)$ in Eq. (3) represents the impacts of external stresses (applied voltage and temperature are commonly used) on the reliability of a BME capacitor. It is widely known that the time-to-failure (TTF) for MLCCs that is caused by a single failure mode when both V and T are changed from V_1 to V_2 and T_1 to T_2 is the product of the separate acceleration factors:

$$A_{VT} = \frac{t_1}{t_2} = \left(\frac{V_2}{V_1}\right)^n \exp\left[\frac{E_a}{k}\left(\frac{1}{T_1} - \frac{1}{T_2}\right)\right], \quad (6)$$

where n is an empirical parameter that represents the voltage acceleration factors, E_a is an activation energy that represents the temperature acceleration factor, and k is the Boltzmann constant.

This well-known Prokopowicz and Vaskas equation (P - V equation) has proven to be useful in the capacitor industry for testing PME MLCCs at various highly accelerated testing conditions. An average of $n \approx 3$ has been found for the voltage acceleration factor, and an average value of $1 < E_a < 2$ eV is typical for the temperature acceleration factor.

Since only a single failure mode is assumed, the value of β in Eq. (4) should not change over applied stresses. Only the Weibull distribution scale parameter η will change with external stresses. This can be expressed, according to Eq. (6), as

$$\eta(V, T) = \frac{C}{V^n} \cdot e^{\left(\frac{B}{T}\right)}, \quad (7)$$

where C and $B = E_a/k$ are constants.

Due to the relatively high concentration of oxygen vacancies in BME capacitors and the impact of oxygen vacancy electromigration on the reliability of BME capacitors, the acceleration function $AF(V, T)$ of BME capacitors has been found to not always follow the power law with respect to applied voltage as specified in Eq. (6). Mixed failures have often been reported for BME capacitors.

A recent NASA NEPP-funded study that combines the measurement of both TTF and the capacitor leakage current as a function of stress has been developed and practiced to describe the reliability of BME capacitors. A two-stage dielectric wear-out process that initiates with a slow dielectric degradation, followed by a thermally dominated catastrophic breakdown, has been revealed (Figure 3). When the failure criterion is set with respect to a leakage current level, some BME capacitors will reach the failure level with a catastrophic failure, and some will fail prior to the occurrence of a catastrophic dielectric breakdown.

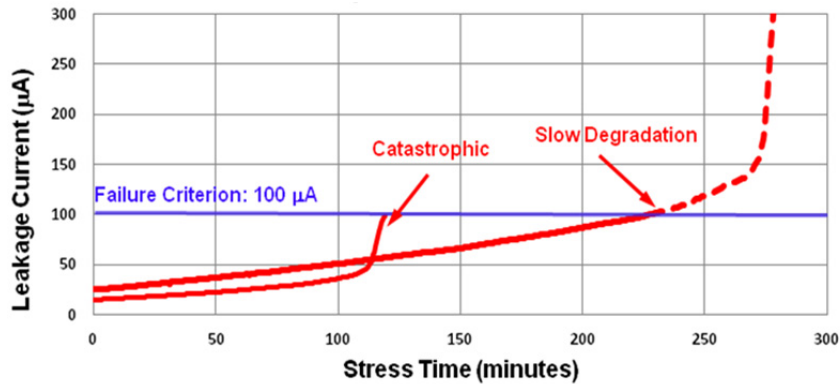


Figure 3. A two-stage dielectric wear-out failure mode is proposed to describe the dielectric breakdown behaviors in BME capacitors.

Further investigation also revealed that the two identified failure modes follow different acceleration functions. Slow degradation fits well to an exponential law against the applied field. The catastrophic failures fit the power-law better. Table I summarizes the two failure modes and corresponding voltage acceleration functions that may be used to model the BME capacitors' reliability life.

Table I. Summary of Acceleration Functions for BME MLCCs

Failure mode	Acceleration function	Expression to scale parameter η	Expression to time-to-failure (TTF)
Slow Degradation	Exponential model	$\eta(E, T) = C e^{-bE} \cdot e^{\left(\frac{E_a}{kT}\right)}$	$\frac{t_1}{t_2} = \exp[-b(E_1 - E_2)] \exp\left[\frac{E_a}{k} \left(\frac{1}{T_1} - \frac{1}{T_2}\right)\right]$
Catastrophic	Power-law (P-V equation)	$\eta(V, T) = \frac{C}{V^n} \cdot e^{\left(\frac{E_a}{kT}\right)}$	$\frac{t_1}{t_2} = \left(\frac{V_2}{V_1}\right)^n \exp\left[\frac{E_a}{k} \left(\frac{1}{T_1} - \frac{1}{T_2}\right)\right]$

4.3 The Impact of Capacitor Structure on the Reliability of BME Capacitors

4.3.1 The Impact of the Number of Dielectric Layers

As shown in Figure 4, a monolithic MLCC can be converted both constructively and electrically to a number of single-layer ceramic capacitors connected in parallel. Assuming C_i is the i -th layer capacitor, the MLCC can be viewed as a parallel connection among $C_1, C_2, C_3, \dots, C_i, \dots, C_N$, where N is the number of dielectric layers inside an MLCC device. Since every single-layer capacitor C_i shares the same electrode area S , the same dielectric thickness d , and the same processing history, it is reasonable to assume that $C_1 = C_2 = C_3 = \dots = C_i \dots = C_N$.

So the sum of the capacitance C_t of an MLCC can be expressed as:

$$C_t = C_1 + C_2 + C_3 \dots + C_i \dots + C_N = N \cdot C_i. \quad (8)$$

Similarly, the reliability of an MLCC with N dielectric layers that are connected in parallel can be expressed as:

$$R_t = R_1 \times R_2 \times R_3 \dots \times R_i \dots \times R_N = R_i^N, \quad (9)$$

where R_i is the reliability of an i -th single-layer capacitor, and R_t is the overall reliability of an MLCC.

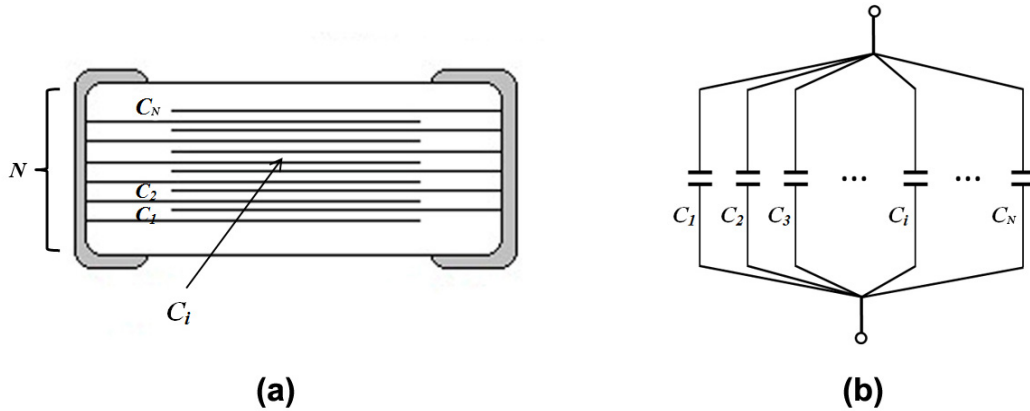


Figure 4. A cross-sectional view of a monolithic MLCC shows a stack of N layers of single-layer capacitors (a); this construction can be equivalently converted to the same number of single-layer capacitors connected in parallel.

The reliability relationship shown in Eq. (9) indicates that the overall reliability R_t of an MLCC device is highly dependent on the reliability R_i of a single-layer capacitor inside a monolithic MLCC body.

From the structure of an MLCC unit shown in Figure 4, capacitor reliability can be expressed as:

$$R_t(t) = R_i(t)^N, \quad (10)$$

where N is the number of individual dielectric layers and $R_i(t)$ is the reliability of a dielectric layer. The capacitor reliability $R_t(t)$ as a function of $R_i(t)$, and N is shown in Figure 5.

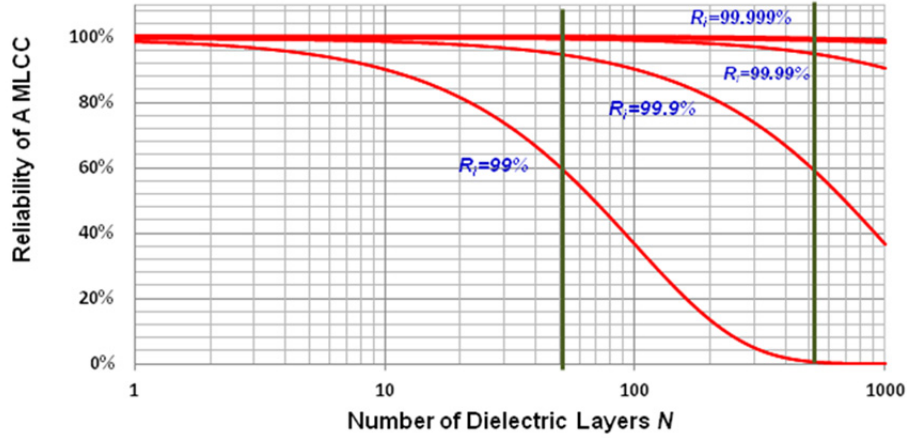


Figure 5. MLCC reliability $R_t(t)$ as a function of dielectric reliability $R_i(t)$ and number of dielectric layers N .

In general, when dielectric reliability $R_i(t)$ is very close to unity, N does not have a significant impact on MLCC reliability $R_t(t)$. If $R_i(t)$ is reduced slightly, the overall reliability $R_t(t)$ of an MLCC can degrade rapidly due to the amplifying effect of the number of dielectric layers N . Since most commercial BME capacitors are made with a large number of dielectric layers (typically $N > 250$), the impact of N on BME capacitor reliability is critical.

4.3.2 The Impact of Number of Grains per Dielectric Layer

As shown in Figure 6, if a single-layer capacitor C_i has an average grain size \bar{r} and an average dielectric thickness d , the number of grains per dielectric layer can be calculated as $\left(\frac{d}{\bar{r}}\right)$.

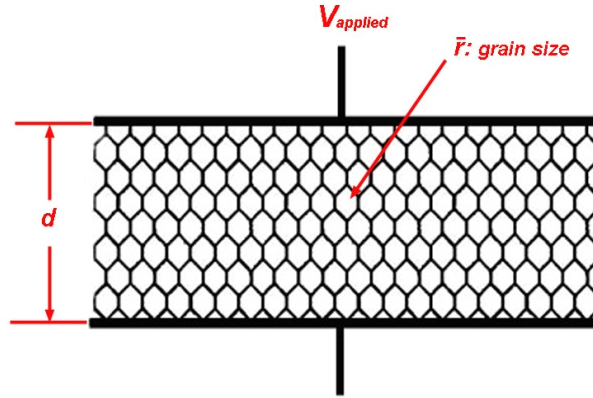


Figure 6. Estimate of the number of grains in a dielectric layer; with average dielectric thickness d and average grain size \bar{r} , the number of grains per dielectric layer can be calculated as $\left(\frac{d}{\bar{r}}\right)$.

The MTTF of BME capacitors as a function of parameter $\left(\frac{d}{\bar{r}}\right)$ was measured and reported recently by Murata (http://iopscience.iop.org/1757-899X/18/9/092007/pdf/1757-899X_18_9_092007.pdf). Figure 7 shows MTTF data (as presented by time dependence of insulating resistance) under high temperature (150°C) and high DC field (10 kV/mm) using highly accelerated life test (HALT). The measured MTTF data are proportional to the number of grains $\left(\frac{d}{\bar{r}}\right)$. But if the voltage per grain boundary is adjusted to a same value, all four MLCCs with different $\left(\frac{d}{\bar{r}}\right)$ values have almost identical MTTF values. According to Eqs. (5) and (7), the MTTF of a BME capacitor at a given temperature can be written as:

$$MTTF = \frac{1}{V_{grain}^n} = \frac{1}{\left[\frac{V_{applied}}{\left(\frac{d}{\bar{r}}\right)}\right]^n} = \frac{1}{V_{applied}^n} \times \left(\frac{d}{\bar{r}}\right)^n \quad (11)$$

This indicates that the MTTF of BME capacitors follows a power-law relationship to the dielectric thickness d when applied voltage and average grain size are both given.

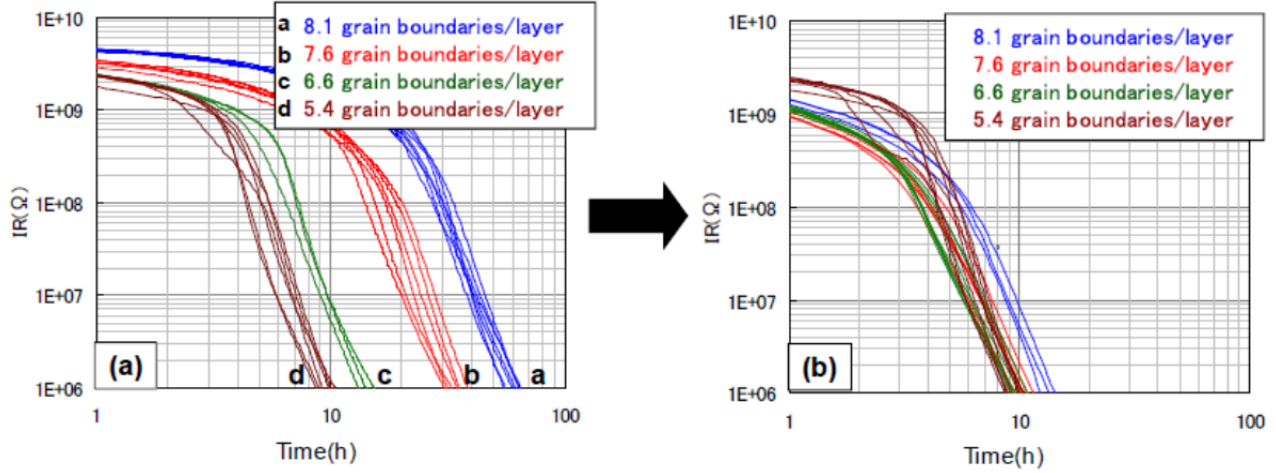


Figure 7. MTTF of BME capacitors as a function of grain boundaries per dielectric layer $\left(\frac{d}{\bar{r}}\right)$. Longer MTTF will be obtained for MLCCs with higher $\left(\frac{d}{\bar{r}}\right)$ values (left); when the applied voltage is adjusted to a constant voltage per grain boundary, MTTF values become identical (test results courtesy of Murata).

In order to implement the microstructure parameter $\left(\frac{d}{\bar{r}}\right)$ into the reliability of a single-layer capacitor, a structural model based on the dielectric thickness and the feature size of a defect can be developed. This model is briefly described below.

As shown in Figure 8, assuming that the feature size of a defect that causes a catastrophic failure is r , d is the dielectric thickness, and the reliability of the defect is 0, then the reliability of a single dielectric layer $R_i(t)$ with thickness d will be determined by the value of d with respect to r . When d is far greater than the defect feature size r , the defect is non-harmful and may not cause any failures for many years, or even during a capacitor's lifetime.

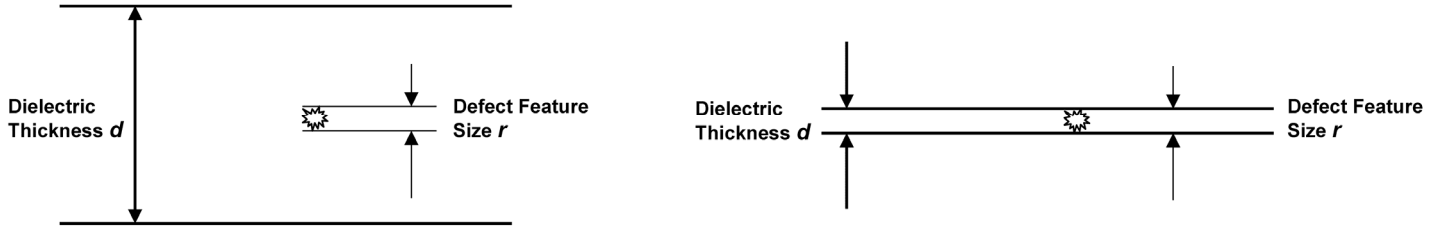


Figure 8. An illustration of dielectric thickness d with respect to feature size r of an extrinsic defect inside the dielectric layer. The dielectric layer reliability is dependent on the ratio r/d : (a), $d \gg r$ (b), $d \approx r$.

However, as d approaches the feature size of the defect r , the defect will cause dielectric failure instantly. In other words, the survival probability of the dielectric layer R_i can be written as $R_i(t) \rightarrow 1$ when $d \gg r$ and as $R_i(t) \rightarrow 0$ when $d \approx r$. According to Eq. (11), the Weibull reliability of a dielectric layer with respect to its thickness d and defect feature size r can thus be expressed as:

$$R_i(t) = e^{-\left(\frac{t}{\eta}\right)^\beta} \cdot \left[1 - \left(\frac{r}{d}\right)^\xi\right].$$

For simplicity, the defect size r can be directly related to the average grain size \bar{r} as: $r \approx c \times \bar{r}$, where c is a constant. The equation above can be further expressed with respect to average grain size \bar{r} as:

$$P = \left[1 - \left(\frac{r}{d}\right)^\xi\right] = \left[1 - \left(\frac{\bar{r}}{d}\right)^\alpha\right], \quad (\alpha \geq 5), \quad (12)$$

where P is a geometric factor that determines the dielectric layer reliability $R_i(t)$ with respect to the microstructure of an MLCC. α is an experimental constant that was determined by the formulation, processing conditions, and microstructure of a BME capacitor. α was determined in this study such that $\alpha \approx 6$ for $V \leq 50$ V and $\alpha \approx 5$ for $V > 50$ V.

The Weibull reliability of a BME capacitor is equal to unity when $t < \eta$, so the reliability of a single dielectric layer inside of an MLCC can be expressed as:

$$R_i(t < \eta) = e^{-\left(\frac{t}{\eta}\right)^\beta} \cdot \left[1 - \left(\frac{\bar{r}}{d}\right)^\alpha\right] = 1 \cdot \left[1 - \left(\frac{\bar{r}}{d}\right)^\alpha\right] = \left[1 - \left(\frac{\bar{r}}{d}\right)^\alpha\right]. \quad (13)$$

Combining Eqs. (10) and (13) yields the time-independent, simplified reliability of a BME MLCC:

$$R_t(t < \eta) = R_i(t < \eta)^N = \left[1 - \left(\frac{\bar{r}}{d}\right)^\alpha\right]^N, \quad (\alpha \geq 5). \quad (14)$$

4.3.3 The Impact of Chip Sizes

In order to reveal the impact of chip size on the reliability of BME MLCCs, the effective areas of MLCC devices with different chip sizes have been measured and normalized with respect to the Electronic Industries Alliance (EIA) chip size of 0402, the smallest chip size used in this comparison study. Corresponding measured results are summarized in Table II. The chip size scaling factor S represents how many times larger the effective area of a given EIA chip size is than that of 0402 for a single dielectric layer. For example, the effective chip size of a 0805 MLCC is equal to 6.76 times that of an 0402 MLCC connected in parallel.

Per Figure 2, Table II, and Eq. (9), the single dielectric layer reliability of a 0805 MLCC $R_i(0805)$ can thus be expressed with respect to that of a 0402 MLCC $R_i(0402)$ as:

$$R_i(0805) = R_i(0402)^{6.76}$$

Table II. EIA Chip Size and Calculated Scaling Factors for BME Capacitors

Chip size	Length (μm)	Width (μm)	Terminal-t (μm)	Side margin (μm)	End margin (μm)	Effective area of a single dielectric layer (mm^2)	Chip size scaling factor S
0402	1000 \pm 100	500 \pm 100	250 \pm 150	125	100	0.225	1.00
0603	1600 \pm 150	810 \pm 150	350 \pm 150	175	100	0.763	3.39
0805	2010 \pm 200	1250 \pm 200	500 \pm 200	250	150	1.520	6.76
1206	3200 \pm 200	1600 \pm 200	500 \pm 200	250	150	3.510	15.60
1210	3200 \pm 200	2500 \pm 200	500 \pm 200	250	150	5.940	26.40
1812	4500 \pm 300	3200 \pm 200	610 \pm 300	300	200	10.920	48.53
2220	5700 \pm 400	5000 \pm 400	640 \pm 390	320	220	23.074	102.55
1825	4500 \pm 300	6400 \pm 400	610 \pm 360	300	220	23.244	103.31

In general, when the chip size scaling factor S is used, the single dielectric layer reliability of an MLCC with an EIA chip size of xy can be expressed with respect to the single dielectric layer reliability of a 0402 MLCC as:

$$R_i(xy) = R_i(0402)^S \quad (15)$$

When the chip size scaling factor increases by a hundredfold, the single dielectric layer reliability declines: 45% when $R_i(0402) = 99\%$; 10% when $R_i(0402) = 99.9\%$; and 1% when $R_i(0402) = 99.99\%$. The single dielectric layer reliability of MLCCs decreases with increasing chip size, but not significantly in comparison to the reliability decrease that accompanies an increase in the number of dielectric layers. Results are shown in Figure 9.

Furthermore, according to Eq. (10), the reliability of an MLCC with chip size xy $R_t(xy)$ can be expressed as:

$$R_t(xy) = [R_i(0402)^{N_{xy}}]^S = \left[R_t(0402)^{\frac{N_{xy}}{N_{0402}}} \right]^S, \quad (16)$$

where $R_t(xy)$ is the reliability of an BME MLCC with a chip size of xy and N_{xy} of dielectric layers; and $R_t(0402) = R_i(0402)^{N_{0402}}$ is that with an 0402 chip size and N_{0402} of dielectric layers. The construction analysis of BME capacitors has revealed that $N_{0402} \approx 70-80$ and $N_{xy} \approx 250-300$, so that $\frac{N_{xy}}{N_{0402}} \approx 3-4$.

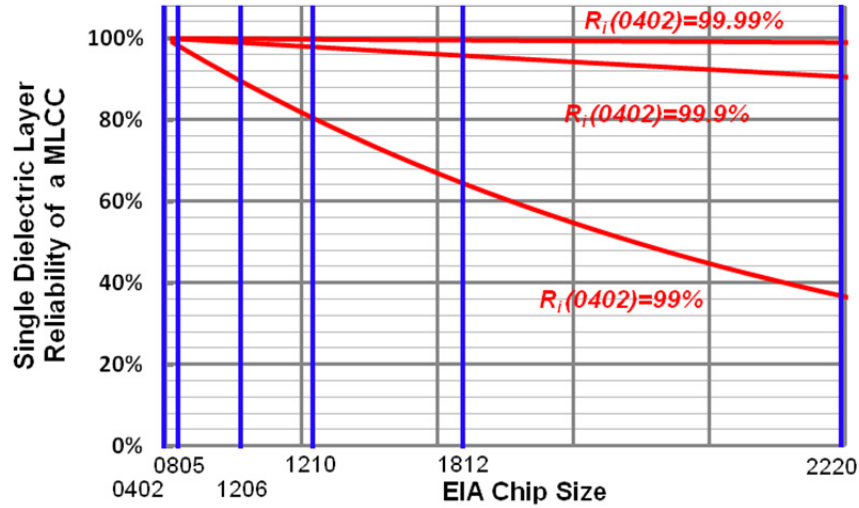


Figure 9. The single dielectric layer reliability $R_i(xy)$ as a function of EIA chip size, and the single layer reliability of a 0402 MLCC $R_i(0402)$.

Conversely, the dielectric thickness of BME capacitors is also found to gradually increase with MLCC chip size. Figure 10 shows the construction analysis results of average BME dielectric thickness as a function of chip size. According to Eq. (11), the MTTF of an MLCC follows a power-law increase with increasing dielectric thickness. Therefore, the reliability decreases due to increasing chip size have been fully compensated for by increasing the dielectric thickness.

As a result of that, the overall reliability of a BME MLCC will not change significantly with increasing capacitor chip size.

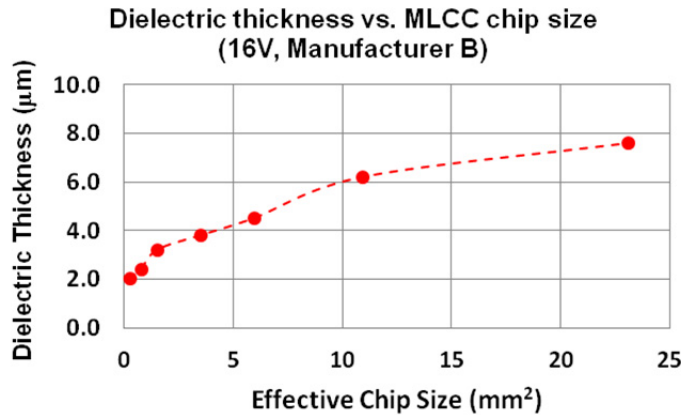


Figure 10. Measured average dielectric thickness as function of BME MLCC chip size.

5. Summary

The general expression of a BME capacitor's reliability given in Eq. (3) can be specifically rewritten for BME capacitors based on this study. A two-parameter Weibull distribution is applicable to $\gamma(t)$. Two identified failure modes will follow different acceleration functions $AF(V, T)$, as summarized in Table I. Function $\varphi(N, d, \bar{r}, S)$ can be expressed using Eq. (14). The impact of chip size S on the reliability of BME capacitors is negligible. Therefore, the reliability of a BME capacitor is finally obtained:

$$R(t) = \varphi(N, d, \bar{r}, S) \times AF(V, T) \times \gamma(t)$$

$$= \left[1 - \left(\frac{\bar{r}}{d} \right)^{\alpha} \right]^N \times \left\{ p \times e^{-\left[\frac{t}{\sqrt{N} \cdot e^{\left(\frac{E_{a1}}{kT} \right)}} \right]^{\beta_1}} + (1-p) \times e^{-\left[\frac{t}{C e^{-bE} \cdot e^{\left(\frac{E_{a2}}{kT} \right)}} \right]^{\beta_2}} \right\},$$

where β_1 and β_2 are the Weibull slope parameters for catastrophic and slow degradation failures, respectively; E_{a1} and E_{a2} are the activation energies for the two failure modes, respectively; p the percentage of catastrophic failures; A , b , C are constants; α is a constant that can be determined experimentally; and N , d , and \bar{r} are the number of dielectric layers, average dielectric thickness, and average grain size, respectively.

6. NASA NEPP-Funded Studies on BME Capacitors

The NASA NEPP program began funding the evaluation of BME capacitors as early as 2004. Following are selected publications on the evaluation of BME capacitors, including a recently released publication entitled “Selection, Qualification, Inspection, and Derating of Multilayer Ceramic Capacitors with Base-Metal Electrodes.” These publications can be accessed via the web links provided. Detailed discussions on the reliability of BME capacitors and other related issues can be found in these published technical papers.

1. J. Brusse and M. Sampson, “COTS Ceramic Chip Capacitors: An Evaluation of the Parts and Assurance Methodologies,” *CARTS Proceedings*, San Antonio, TX, pp. 128–140, (2004). (<http://nepp.nasa.gov/DocUploads/65B2E69A-658E-46EE-BF080EAB54B25EDC/2004%20Brusse-COTS%20Ceramic%20Caps%20-%20An%20Eval%20Report.pdf>)
2. D. Liu, H. Leidecker, T. Perry, and F. Felt, “Accelerating Factors in Life Testing of High-Voltage Multilayer Ceramic Capacitors,” *CARTS Proceedings*, Palm Springs, pp. 151–156, (March 21–24, 2005). (ecadigitallibrary.com/pdf/CARTS50551_05ijt.pdf)
3. D. Liu and M. Sampson, “Reliability Evaluation of Base-Metal-Electrode Multilayer Ceramic Capacitors for Potential Space Applications,” *CARTS Proceedings*, pp. 45–63, (2011). (https://nepp.nasa.gov/files/21703/GSFC_Liu_Sampson_Reliability_Eval_BME_Multilayer_Ceramic.pdf)
4. D. Liu, “Failure Modes in Capacitors When Tested Under a Time-Varying Stress,” *CARTS Proceedings*, pp. 209–223, (2011). (https://nepp.nasa.gov/files/21705/11_005_gsfc_Liu_Failure_Modes_in_Capacitors.pdf)
5. D. Liu and M. J. Sampson, “Some Aspects of the Failure Mechanisms in BaTiO₃-Based Multilayer Ceramic Capacitors,” *CARTS Proceedings*, Las Vegas, NV, pp. 59–71, (March 26–29, 2012). (*CARTS Outstanding Paper Award*) (https://nepp.nasa.gov/files/24291/CARTS2012_Liu_BaTiO3.pdf)
6. D. Liu, “Evaluation of Multilayer Ceramic Capacitors with C0G Dielectric and Base-Metal Electrodes,” *NASA NEPP FY Report*, Part II, NEPP Task 1051-005, GSFC, Greenbelt, MD, (2012). (https://nepp.nasa.gov/files/24320/Liu_2013_Pt2Capacitors.pdf)
7. D. Liu, “Highly Accelerated Life Stress Testing (HALST) of Base-Metal Electrode Multilayer Ceramic Capacitors,” *CARTS Proceedings*, Houston, TX, pp. 235–248, (March 26–29, 2013). (https://nepp.nasa.gov/files/24300/CARTS2013_Liu_HALST.pdf)
8. R. Weachock and D. Liu, “Failure Analysis of Dielectric Breakdowns in Base-Metal Electrode Multilayer Ceramic Capacitors,” *CARTS Proceedings*, Houston, TX, pp. 151–165, (2013). (https://nepp.nasa.gov/files/24303/CARTS2013_Liu_FailureAnalysis.pdf)
9. D. Liu, “Selection, Qualification, Inspection, and Derating of Multilayer Ceramic Capacitors with Base-Metal Electrodes,” *NASA NEPP FY Report*, (2013). (https://nepp.nasa.gov/files/24351/Liu_2013_G11_BME_Guidelines.pdf)

For more information, contact

David (Donhang) Liu at 301-286-8573

GIDEP Alerts/Advisories

Contact your GIDEP Representative for a copy of:

Suspect Counterfeit	CHZ-A-13-01 Disk Drive Unit, CHZ-A-13-02 Disk Drive Unit, CHZ-A-13-03 Disk Drive Unit, D8Y-A-13-06 4-Port Gigabit and 24-Port Ethernet Switch/Router, D8Y-A-13-07A, Unprogrammable parts, Highly Programmable Voltage Supervisory Circuit, D8Y-A-13-08A Suspect Counterfeit, Microcircuit, 32Kx8 Autostore nvSRAM, GR2-P-13-01 Transistor, Silicon PNP, 6 Watt, R4-A-13-06 Microcircuit, Op-Amp, 1000 uV Offset-Max, 725 MHz Band Width
Misc.	EK-S-13-01 Connector, Plug, Electrical, EO-P-13-01 Samarium Cobalt (SmCo) Specialty Metal High Performance Magnet, GB4-P-13-02A Microcircuit, Digital, CMOS, Radiation Hardened, 32-BIT Fault-Tolerant Processor, Monolithic Silicon, GB4-P-13-03 Microcircuit, Memory, Digital, CMOS, Radiation Hardened Dual Voltage SRAM, with EDAC, NX4-P-13-01A Contact, Termini, Fiber Optic, Connector, Removable Environment Resisting, Pin/Socket Terminus, SW3-P-13-01 Microcircuit, Digital Driver, High Level

Reduced Schedule of Meetings

(Communication from DLA)

Due to “sequestration” and other budgetary negotiations in Congress and the associated contingency planning at DLA due to these negotiations, all travel that can be deferred will be deferred indefinitely. The publishing of the audit schedule will also be suspended during this time. For the rare exceptions to the travel deferment, you should hear from the responsible engineer/technician or Branch Chief directly. If you have any questions, please direct them to Joe Gemperline, (614) 692-0663, or Joseph.Gemperline@dla.mil.

NASA Parts Specialists Recent Support for DLA Land and Maritime Audits:

Audit performed at Crane Electronics, Redmond, Washington

Upcoming Meetings

- JEDEC JC-13, Memphis, Tennessee, May 20–23, 2013
- Electronics Technology Workshop (ETW) at GSFC, Greenbelt, Maryland, June 11–12, 2013
<http://nepp.nasa.gov/workshops/etw2013/>
- JEDEC JC-13, Columbus, Ohio, Sept. 16–19, 2013
Space Passive Component Days, 1st International Symposium, ESA/ESTEC, Noordwijk, the Netherlands, September 24–26, 2013
<http://www.globaleventslist.elsevier.com/events/2013/09/space-passive-component-days/>

Contacts

NEPAG

<http://atpo.jpl.nasa.gov/nepag/index.html>

Shri Agarwal 818-354-5598
Shri.g.agarwal@jpl.nasa.gov

Roger Carlson 818-354-2295
Roger.v.carlson@jpl.nasa.gov

Lori Risse 818-354-5131
Lori.a.risse@jpl.nasa.gov

ATPO <http://atpo.jpl.nasa.gov>

Chuck Barnes 818-354-4467
Charles.e.barnes@jpl.nasa.gov

JPL Electronic Parts <http://parts.jpl.nasa.gov>

Rob Menke 818-393-7780
Robert.j.menke@jpl.nasa.gov

Previous Issues:

JPL: <http://atpo/nepag/index.html>

Other NASA centers:

<http://nepp.nasa.gov/index.cfm/12753>

Public Link (best with Internet Explorer):

<http://trs-new.jpl.nasa.gov/dspace/handle/2014/41402>

www.nasa.gov

National Aeronautics and Space Administration

Jet Propulsion Laboratory

California Institute of Technology
Pasadena, California

© 2013 California Institute of Technology
Government sponsorship Acknowledged.